Advancements of Extrusion Simulation in DEFORM-3D

By G. Li, J. Yang, J.Y. Oh, M. Foster, and W. Wu, Scientific Forming Tech. Corp.; and P. Tsai and W. Chang, MIRDC

Introduction

It has been widely accepted that the finite element method (FEM) is a powerful numerical tool for the design of extrusion processes and dies, which so far has mainly relied on the expertise of highly experienced designers and costly plant trials. The extruded shapes of light alloys typically have a complex geometry and thin profiles, which necessitate large billet area reduction. Sharp corners are also commonplace in the die structure. These issues pose tough challenges for numerical analysis.

To model the extrusion process with the FEM, three formulations can be used. The transient updated Lagrangian (UL) formulation, where the FEM mesh is attached to the deforming billet, is able to capture the material flow in a very intuitive way. Runtimes can be long, but this method can produce some results that are difficult or impossible to obtain from other simulation methods. Some available results include: material splitting over the bridge and merging in the welding chamber for a hollow extrudate, front end formation, curling or twisting of the entire extrudate, and complete load vs. stroke behavior. Parallel computing can speed up UL simulations. The steady state (SS) Eulerian approach, in which the mesh is fixed in space, is fast but can not provide any transient information and the thermal-mechanical stationarity may not be well established in reality. The ALE (Arbitrary Lagrangian Eulerian) approach falls somewhere between the other two methods. It is efficient for this class of problems,[1,2] since the frequent remeshing inevitable in UL can be eliminated. Also, some of the shortcomings of the SS approach can also be circumvented since the procedure is incremental in nature.

This paper discusses the recent advances in the commercial code DEFORM-3D for extrusion modeling. DEFORM-3D can model all three of the approaches mentioned, but recent efforts have been focused on the improvement of the ALE formulation. This development is intended to provide an efficient numerical tool for extrusion processes, as well as a dedicated template for the preparation of the input data. To validate the code, an industrial example with a hollow profile and several welds was simulated using the three approaches in DEFORM-3D, and the results are compared with the experiments. The flow stress testing and the extrusion experiment are also described.

For further discussions of the three different formulations, as well as the general procedure of the ALE approach, please refers to an earlier paper.[2] This paper summarizes the ALE methodologies for extrusion. An extrusion example used to demonstrate the UL, ALE, and SS methods is given. Finally, comparisons between the FEM predictions and the actual process are made to validate the approaches and demonstrate the capability of the system.

ALE Formulation and Procedure

The ALE method is an attempt to combine the advantages of both the Eulerian and Lagrangian formulations. It was first introduced by Hirt, et al.,[3] and Donea, et al.,[4] in modeling the solid-fluid interaction. It was subsequently applied to problems of solid mechanics with large deformation.[5]

The general ALE method uses two mesh systems: the computational reference mesh system (CRS), on which the finite element calculations are performed, and the material reference mesh system (MRS), which follows the material as it deforms. The relationship between the CRS and MRS in each of the Lagrangian, Eulerian, and ALE descriptions is shown in Figure 1. At the beginning of a new ALE step, the MRS mesh is made to be the same as the CRS mesh. In a time increment, the nodes move together with the material for the Lagrangian formulation. For the Eulerian formulation, the nodes are fixed in space. For the ALE method, the new position of the CRS nodes can be designed based on the need of the simulation.

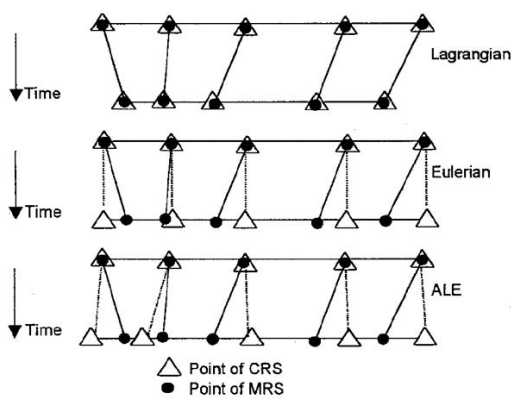

Figure 1. Relationship between CRS and MRS using different formulations.

In the DEFORM-3D ALE formulation, both MRS and CRS consist of hexahedral or tetrahedral elements that are moving in the extrusion direction. The movement of the CRS differs in the three directions. The nodes are fixed in the extrusion direction, while they are updated in a Lagrangian fashion in the plane perpendicular to the extruding direction. To implement this, the CRS is superimposed with the MRS at the beginning of the simulation. The increment proceeds exactly as that for the pure Lagrangian description using the CRS through the end of the solution phase. As the computational mesh deforms and changes its geometry, new coordinates and deformation state variables are obtained during the simulation and then are transferred to the MRS at the end of each increment to update it. The CRS remains unchanged at this stage. Since the initial nodes and elements of the computational mesh belong to the material mesh, no interpolation of the state variables is needed. Instead, nodal and elemental values are simply registered to the material mesh.

After MRS updating, it is necessary to update the CRS to obtain a mesh whose boundary coincides with that of the updated MRS, but whose nodes retain their position along the extrusion direction. Generally the CRS nodal updating is done by projection onto the MRS surface. But, due to discretization, the MRS surface is not smooth when the curvature is not zero. Consequently the nodes

cannot be moved on the surfaces without destroying the original shape of the surface. To deal with this problem, a spline surface on the MRS mesh is generated. Figure 2 shows a surface mesh around a CRS node before the update. The new position of the CRS node is projected onto this spline surface.

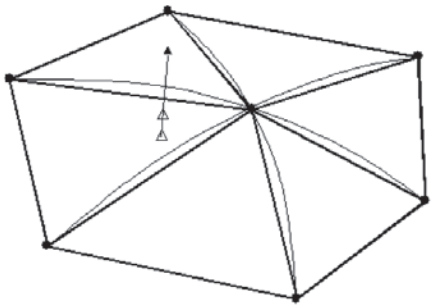

Figure 2. A CRS node projection on the MRS surface.

The updated CRS and MRS are no longer superimposed at this point. However, after the updated CRS is obtained from the updated MRS, the latter can be discarded. The simulation of the next incremental step uses the updated CRS and finishes with a new updated MRS. With this ALE mesh design and updating scheme, a stable contact definition between the billet and the dies is maintained.

State Variable Update: In the ALE procedure, it is necessary to update the state variables when mapping them from the MRS to the CRS. Theoretically, the convection of the state variables, say, the effective strain, is based on:

$$\frac{\partial_{CRS}\varepsilon}{\partial t} = \dot{\varepsilon} - (\mathbf{v} - \mathbf{v}_{CRS}) \cdot \nabla \varepsilon \qquad (1)$$

Difficulty arises when calculating the gradient terms of the elemental state variables, as they are defined at the integration point(s) of each element and are therefore only piecewise continuous. Two approaches can be found in the literature: interpolation and convection. The interpolation method updates the nodal coordinates as well as the state variables in the MRS, and then maps the state variables to the CRS.[6] The convection method solves Eq. (1) to update the state variables. The Godunov-type update proposed by Rodriguez-Feran, et al.,[7] belonging to the second group, is used in this work. To obtain the effective strain of a particular element with respect to the CRS, a surface integration containing a flux is considered by:

$$\varepsilon_{n+1} = {}^{L}\varepsilon - \frac{\Delta t}{2V}\sum_{\Gamma=1}^{N_\Gamma} f_\Gamma(\varepsilon_\Gamma^c - \varepsilon)[1 - sign(f_\Gamma)] \qquad (2)$$

Where ε_{n+1} is the convected strain with respect to the CRS. The variable ${}^{L}\varepsilon$ is the material strain and N_Γ is the total number of the surfaces Γ between this element, with volume V, and the contiguous elements, whose strain is denoted by the superscript ^{c}. Also required for the calculation is

$$f_\Gamma = \int_\Gamma \mathbf{c} \cdot \mathbf{n} d\Gamma \quad \text{Where } \mathbf{c} = \mathbf{v} - \mathbf{v}_{CRS}. \qquad (3)$$

As pointed out by Rodriguez-Feran, et al., the time step Δt should not be too large as to bring a particle to cross an entire element at the speed of the convective velocity c. Figure 3 shows some examples of ALE simulations. The profiles were designed to show the capability of predicting extrudate distortion.

Industrial Example

An industrial extrusion profile used for this simulation is shown in Figure 4. Since the profile has a plane of symmetry, only one half was used in the simulation. The material was AA 6061 with an initial billet temperature of 460°C and a ram speed of 33.3 mm/sec. In the die design, there were three mandrels (for the half model) attached to the die body with bridges to form the three holes. During extrusion, the aluminum flows over the bridges into the port holes, where it splits and then merges together in the welding chamber. As a result, there are seven welding seams in the half extrudate.

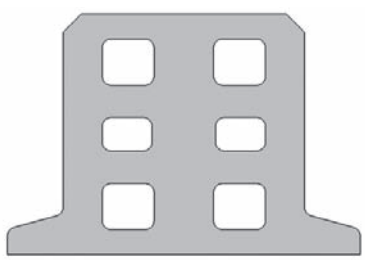

Figure 4. Industrial extrusion profile.

Steady State Simulation: An FEM mesh was created based on the shape derived from the die geometries. It was assumed that the material completely filled up the die cavities and the welds were formed so the extruded section was an integral one. Varying element sizes were used in different regions, with the finest elements defined around the die orifices (Figure 5).

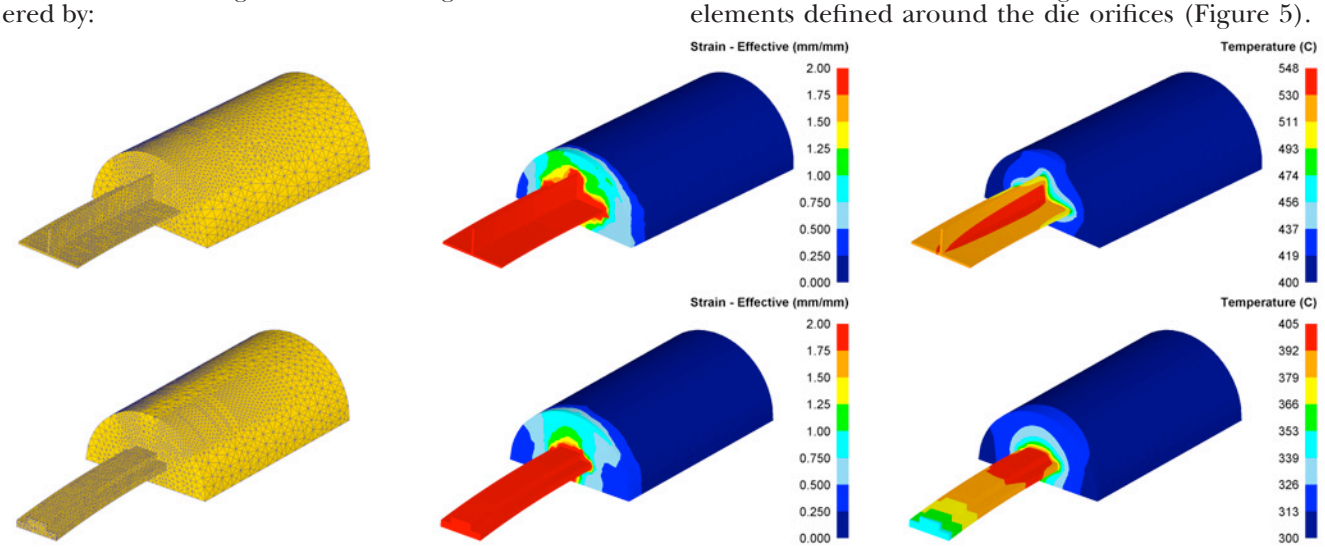

Figure 3: ALE simulation examples. Top Row: T-shaped; Bottom Row: step-shaped.

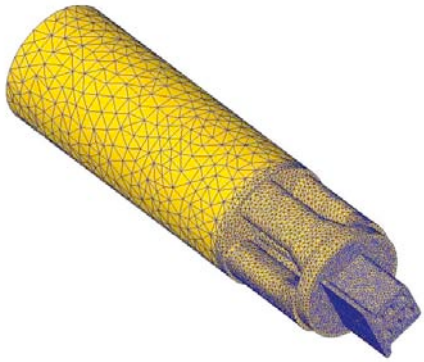

Figure 5. FEM mesh used for the SS/ALE simulations.

In this way, the deformation details were captured more accurately and the computation resources were utilized more effectively.

When setting up the simulation, the flow stresses were first input from an existing material library. The friction factor at the interface between the billet and container was set to 1, while 0.4 was used on the die surface and bearing channel. The SS simulation was run until the deformation reached a steady state solution. At that time, nodal velocities, temperatures, and elemental strains of the billet were obtained. The extrudate distortion was also calculated. Due to the bulky profile shape and the appropriate bearing design, no significant distortion was found in the results. The predicted extrusion load was 181.2 SI tons at the billet length of 160 mm, which was lower than the experimental results. Upon investigation, it was found that the flow stress data was not accurate. Flow stress testing was performed, and the predicted load using the new flow stress data was 336 SI tons.

Updated Lagrangian Simulation: The updated Lagrangian simulation was run from the beginning of the extrusion process, with the starting workpiece being an undeformed 160 mm tall cylindrical billet. The same material and processing conditions described below for the extrusion experiment were used in the simulation.

Figure 6 shows the stages of the UL simulation. At the start of the process, the billet was compressed in the container and the five legs were extruded. The outer legs were longer than the inner leg at this point. These five legs then entered the welding chamber where the four outer flows converged. During this process, the flow of these outer legs was impeded and the inner leg was allowed to freely extrude. For this reason, the central leg ended up longer than the outer four. The press load increased substantially as the welding chamber filled, and the extrudate began to form. The internal ribs were the final feature of the cross-section to form as the extrudate came out of the die.

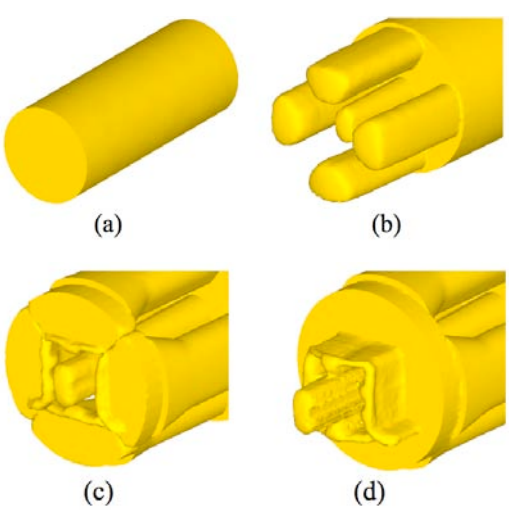

Figure 6. Stages of the UL extrusion simulation: (a) initial billet, (b) extrusion of legs, (c) material in welding chamber, (d) final extrudate formation.

In an updated Lagrangian extrusion simulation, the workpiece mesh deforms and extrudes through the dies. Due to the extensive deformation at the die corners, remeshing of the workpiece was a common occurrence. Self-contact of the merging flows in the welding chamber also contributed to remeshing. When the four outer flows had essentially merged in the welding chamber, the self-contacting surfaces between the flows were manually removed to speed up the simulation (Figures 7-8).

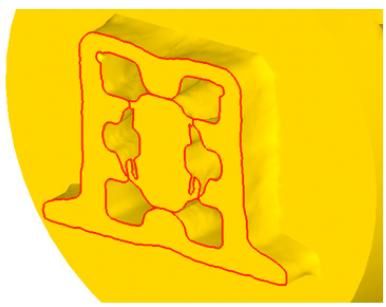

Figure 7. Cross-section showing weld seams in extrudate.

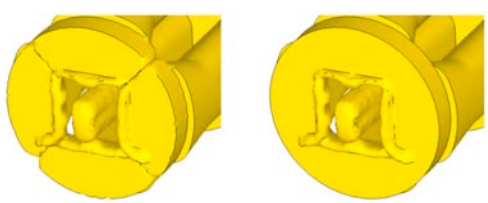

Figure 8. These self-contacting weld seams were manually removed to speed up the simulation.

Figure 9(a) shows the load on the ram as a function of ram stroke. The load is relatively constant at the start of the process when the legs are freely extruding. As the material gets to the welding chamber, the load increases significantly. This simulation was run to the point shown in Figure 6(d). At this point, the extrudate shape has almost reached its steady-state shape. At the end of the simulation, the load has leveled off at ~285 SI tons. Figure 9(b) compares the experimental and UL simulated extrusion loads. Given the experimental loads of 220 SI tons (100 mm billet) and 350 SI tons (200 mm billet), the simulated load of 285 SI tons (160 mm billet) is quite reasonable. It is noted that billet lengths in the UL simulation and experiment are different since the actual billet length was not decided at the time of the simulation.

Incremental ALE Simulation: The ALE simulation was run with the same mesh system as used in the SS simulation. Figure 10 shows the predicted shape after running 1,000 steps. As with the steady state result, no significant distortion was found in the predicted extrudate shape. The predicted effective strain is shown in Figure 11 and the predicted temperature distribution is shown in Figure 12. A load of 146 SI tons was predicted in the half model simulation. Figure 9(a) shows that the corresponding full model load of 292 SI tons matches well with the load predicted at the end of the UL simulation.

Flow Stress Test and Extrusion Experiment

Flow Stress Test: A Gleeble-3500 was used to get accurate flow stress curves for AA 6061. The specimens had an OD

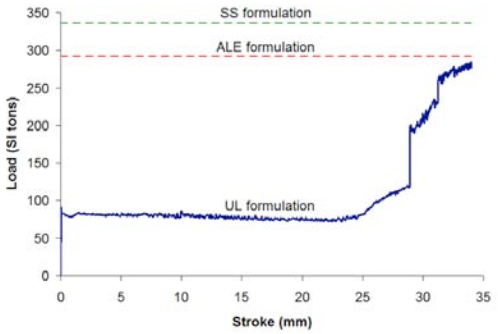

(a)

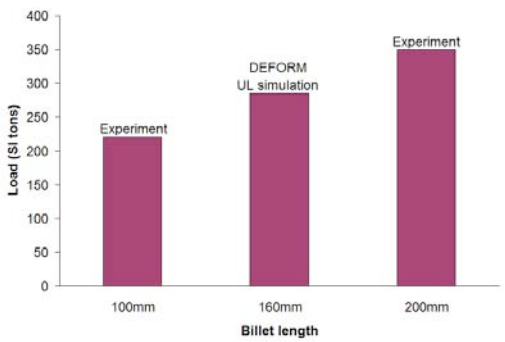

(b)

Figure 9. Load prediction: (a) comparison of three DEFORM formulations, (b) comparison between DEFORM and experimental results.

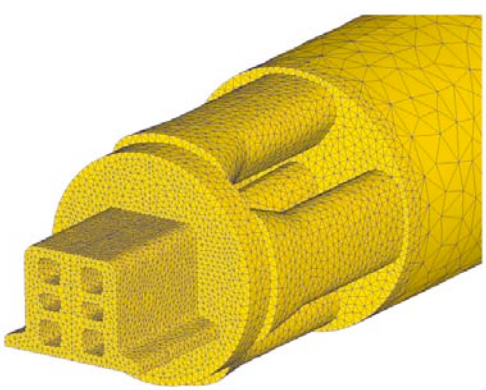

Figure 10. Extrudate shape prediction (ALE).

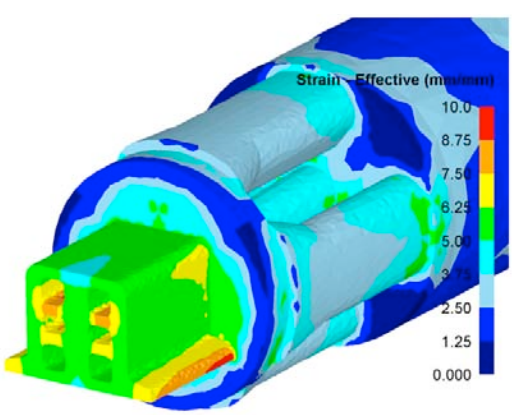

Figure 11. Effective strain prediction (ALE).

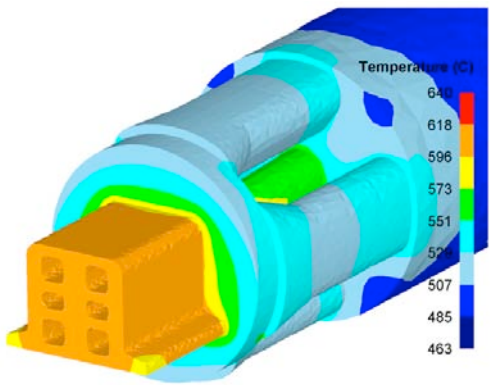

Figure 12. Temperature prediction (ALE).

of 8 mm and a length of 12 mm. Testing conditions are shown in Table I. The flow stress curves obtained from the tests were functions of temperature, strain, and strain rate. These curves were imported into DEFORM-3D for use in the simulations.

AL 6061		Temperature (°C)		
		400	480	560
Strain Rate	0.1	A	B	C
	5	D	E	F
	50	G	H	I

Table I. Gleeble testing conditions.

Extrusion Experiment: An extrusion experiment was performed for comparison with the simulated results. A 350-ton forward extrusion press was used (Figure 13). Table II shows the experimental conditions. Two initial billet lengths were used in the experiment. The maximum load for the 100 mm billet was 220 SI tons, while the max load for the 200 mm billet was 350 SI tons. The billet length directly affects the friction with the container wall. Often, shorter billets are preferred in real applications in order to control the load, temperature distribution, quality, etc. Figures 14 and 15 are photos of the extrudate taken in the experiment. The slightly burgeoning shape is seen at the front end, and the welding lines are clear. The cross-section was quite uniform when it reached steady state extrusion.

Figure 13. 350-ton forward extrusion press

Billet Size	Diameter: 63.5 mm Length: Billet A: 100 mm Billet B: 200 mm
Temperatures	Billet: 460°C Dies: 430~440°C Ram: 460°C Container: 400°C
Ram Speed	33.3 mm/sec

Table II. Extrusion experimental conditions.

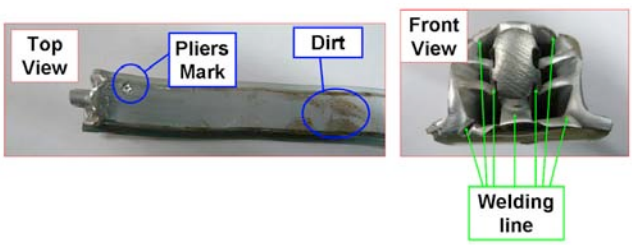

Figure 14. Front end of extrusion.

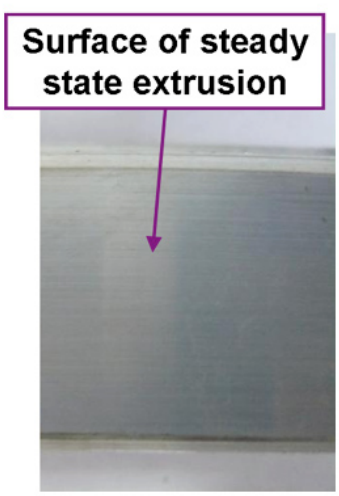

Figure 15. Surface of steady state extrusion.

Comparison and Discussion

Figure 9 shows that the three simulation approaches (SS, ALE, and UL) show good agreement with one another with regard to steady state load prediction. Figure 10 confirms that the predicted load correlates well with the loads obtained from the extrusion experiments. This good correlation between simulated and experimental loads shows the importance of using accurate flow stress input data.

The UL approach has been proven to be a valid tool in providing detailed material flow information in extrusion such as the front-end formation and the weld seam evolution. At the front end of the simulated extrudate, the central leg is longer than the surrounding profile, which matches the observation in experiment. The burgeoning shape of the surrounding profile at the front-end can also be seen in the simulation results. With the self-contact techniques, the merge of the material counter-flows can be modeled and the weld strength can be tracked, although in this simulation the self-contact was removed after some remeshing to speed up the simulation. The capability to provide the material flow details of this method shows its potential in the analysis of flow-induced extrusion defects.

The ALE approach has been improved to more accurately capture the free surface deformation of the extrudate. Since no remeshing is needed, design changes to the bearing channel can be efficiently simulated to help minimize extrudate distortion. In terms of the simulation time, the SS simulation took less than two hours (using a single core on AMD Athlon 64x2 dual core), the ALE took ten hours (Xeon 5160 using four out of the six cores), and the UL took 126 hours (Intel Core i7 920 using four cores).

In this paper, the advantages of FEM technique in accurately predicting extrusion loads and deformed extrudate have been demonstrated and validated by an industrial extrusion example. Future effort will include more validations, and further improvement in the areas of the user friendliness, computational efficiency, and coupling of micro-structure and thermal-mechanical models.

Editor's Note: For more information, contact G. Li by email at: gli@deform.com.

References

1. Belytschko, F., W.K. Liu, and B. Moran, *Nonlinear Finite Elements for Continuous and Structures*, John Wiley & Sons. 2000.

2. Li, G., W. Wu, P. Chigurupati, J. Fluhrer, and S. Andreoli, "Recent Advancement of Extrusion Simulation in DEFORM-3D," Latest Advances in Extrusion Technology and Simulation in Europe, Bologna, Italy, 2007.

3. Hirt, C., A. Amsden, and J. Cook, "An arbitrary Lagrangian-Eulerian computing method for all flow speeds," *Journal of Computational Physics*, 14/3:227-253, 1974.

4. Donea, J., P. Fasoli-Stella, and S. Giuliana, "Lagrangian and Eulerian finite element techniques for transient fluid-structure interaction problem," *Transactions of 4th International Conference on SMIR*, pp. 1-12, 1977.

5. Haber, R., "A mixed Eulerian-Lagrangian displacement model for large deformation analysis inb solid mechanics," *Computer Methods in Applied Mechanics and Engineering*, 43:277-292, 1984.

6. Zienkiewicz, O.C. and J.Z. Zhu, "The Superconvergent Patch Recovery (SPR) and adaptive finite element," *Computer Methods in Applied Mechanics and Engineering*, 101:207-224, 1992.

7. Rodriguez-Feran, A., F.M. Casadei, and A. Huerta, "ALE stress update for transient and quasistatic," *International Journal for Numerical Methods in Engineering*, l.41:241-262, 1998.